Cell Death and Differentiation (2011) 18, 1651–1663

www.nature.com/cdd

Intracellular zinc release-activated ERK-dependent GSK-3β–p53 and Noxa–Mcl-1 signaling are both involved in cardiac ischemic-reperfusion injury

This article has been corrected since Advance Online Publication and a corrigendum is also printed in this issue

C-L Lin[1,2,5], H-C Tseng[1,5], R-F Chen[2,5], W-P Chen[3,5], M-J Su[3], K-M Fang*[,4] and M-L Wu*[,1]

Oxidative stress and nitrosative stress are both suggested to be involved in cardiac ischemia-reperfusion (I/R) injury. Using time-lapse confocal microscopy of cardiomyocytes and high-affinity $O_2^{-\bullet}$ and Zn^{2+} probes, this study is the first to show that I/R, reactive oxygen species (ROS), and reactive nitrogen species (RNS) all cause a marked increase in the $[O_2^{-\bullet}]_i$, resulting in cytosolic and mitochondrial Zn^{2+} release. Exposure to a cell-penetrating, high-affinity Zn_i^{2+} chelator, TPEN, largely abolished the Zn_i^{2+} release and markedly protected myocytes from I/R-, ROS-, RNS-, or Zn^{2+}/K^+ (Zn_i^{2+} supplementation)-induced myocyte apoptosis for at least 24 h after TPEN removal. Flavonoids and U0126 (a MEK1/2 inhibitor) largely inhibited the myocyte apoptosis and the TPEN-sensitive I/R- or Zn_i^{2+} supplement-induced persistent extracellular signal-regulated kinase 1 and 2 (ERK1/2) phosphorylation, dephosphorylation of p-Ser9 on glycogen synthase kinase 3β (GSK-3β), and the translocation into and accumulation of p-Tyr216 GSK-3β and p53 in, the nucleus. Silencing of GSK-3β or p53 expression was cardioprotective, indicating that activation of the ERK–GSK-3β–p53 signaling pathway is involved in Zn^{2+}-sensitive myocyte death. Moreover, the ERK-dependent Noxa–myeloid cell leukemia-1 (Mcl-1) pathway is also involved, as silencing of Noxa expression was cardioprotective and U0126 abolished both the increase in Noxa expression and in Mcl-1 degradation. Thus, acute upstream Zn_i^{2+} chelation at the start of reperfusion and the use of natural products, that is, flavonoids, may be beneficial in the treatment of cardiac I/R injury.
Cell Death and Differentiation (2011) **18,** 1651–1663; doi:10.1038/cdd.2011.80; published online 10 June 2011

Zinc is an element critical to life and is involved in gene transcription and metalloenzyme function. However, the free form of the ion can be toxic and the intracellular free Zn^{2+} concentration ($[Zn^{2+}]_i$) is tightly regulated by membrane transporters and zinc-binding proteins, including high-affinity zinc-finger proteins and low-affinity cysteine-rich metallothioneins (MTs).[1] Using a ratiometric biosensor, the basal $[Zn^{2+}]_i$ in PC-12 cells has been shown to be in the picomolar range.[2]

Reactive oxygen species (ROS) (H_2O_2, $OH^\bullet$, and $O_2^{-\bullet}$) and reactive nitrogen species (RNS) ($NO^\bullet$ and $ONOO^-$) are involved in several myocardial pathophysiological responses, including ischemia/reperfusion (I/R) injury.[3–5] In an MT-overexpressing transgenic mouse model, the heart was found to be highly resistant to I/R-induced myocardial infarction.[6] There is also evidence that $NO^\bullet$-induced Zn_i^{2+} release in neurons induces cell death, as $NO^\bullet$ leads to $ONOO^-$ (peroxynitrite) formation and consequent Zn_i^{2+} release, followed by opening of the mitochondrial permeability transition pore (mPTP),[7] resulting in neuron and glia apoptosis.[7,8] The molecular mechanism of Zn_i^{2+} release-induced neuronal cell death is not clear, but may involve activation of either p38-K^+ channels or the extracellular signal-regulated kinase (ERK)–lipoxygenase (LOX)–ROS pathway.[7,8]

When a non-acetoxymethyl ester Zn^{2+} indicator, TSQ, is applied to the heart tissues, reperfusion induces a decrease, rather than an increase, in $[Zn^{2+}]_i$ levels.[9,10] When a mixture of Zn^{2+} and the Zn^{2+} ionophore pyrithione is added to the reperfusion solution for 20–30 min, cardioprotection occurs, and two mechanisms have been suggested, namely preservation of protein kinase C (PKC) isoforms and inhibition of mitochondrial metabolism.[9,10] The molecular mechanism for the effect of the $[Zn^{2+}]_i$ increase on cell survival is therefore still debatable.

[1]Institute of Physiology, College of Medicine, National Taiwan University, Taipei, Taiwan; [2]Department of Life Science and Institute of Zoology, National Taiwan University, Taipei, Taiwan; [3]Institute of Pharmacology, College of Medicine, National Taiwan University, Taipei, Taiwan and [4]Department of Dental Technology and Material Science, Central Taiwan University of Science and Technology, Taichung, Taiwan
*Corresponding authors: M-L Wu, Institute of Physiology, College of Medicine, National Taiwan University, No. 1, sec. 1, Jen-Ai Road, Taipei 001, Taiwan. Tel: +88 622 312 3456 extn 88242; Fax: +88 622 322 4330; E-mail: meilin@ntu.edu.tw
or K-M Fang, Department of Dental Technology and Material Sciences, Central Taiwan University of Science and Technology, No. 666, Buzih Road, Beitun District, Taichung City 40601, Taiwan. Tel: +88 642 239 1647 extn 7406; Fax: +88 642 277 5625; E-mail: afangkm@gmail.com
[5]These authors contributed equally to this work.
Keywords: I/R injury; zinc; TPEN; flavonoids; GSK-3β; Noxa
Abbreviations: I/R injury, ischemia/reperfusion injury; ROS, reactive oxygen species; RNS, reactive nitrogen species; Zn_i^{2+}, intracellular free Zn^{2+} ions; TPEN, N,N,N′,N′, tetrakis (2-pyridylmethyl) ethylenediaminepentaethylene; NAC, *N*-acetylcysteine; DTT, dithiothreitol; MT, metallothionein; mPTP, mitochondrial permeability transition pore; PFT-α, pifithrin-α; MEK1/2, kinase mitogen protein kinase kinase 1 and 2; ERK1/2, extracellular signal-regulated kinase 1 and 2; GSK-3β, glycogen synthase kinase-3β; Mcl-1, myeloid cell leukemia-1; LOX, lipoxygenase; NFκB, nuclear factor κB; HIF1α, hypoxia-inducible factor-1; PKC, protein kinase C
Received 17.9.10; revised 15.4.11; accepted 04.5.11; Edited by A Finazzi-Agró; published online: 10.6.11

As the basal $[Zn^{2+}]_i$ is extremely low,[2] an understanding of the role of free zinc in living cells has been hindered by the lack of suitable imaging reagents. Using time-lapse confocal microscopy of cardiomyocytes and two sensitive Zn^{2+}-selective probes FluoZin-3 AM (Kd = 15 nM) and RhodZin3 AM (Kd = 65 nM),[11] this study is the first to show that I/R, ROS, and RNS all cause significant cytosolic and/or mitochondrial Zn_i^{2+} release. The role of altered zinc homeostasis in myocyte survival and the molecular mechanism involved was investigated.

Results

Both ROS and RNS induce intracellular Zn^{2+} (Zn_i^{2+}) release. Both ROS and RNS have been suggested to be involved in cardiac I/R injury.[3–5] We tested whether direct exposure to ROS (e.g. H_2O_2) or RNS (e.g. $ONOO^-$) stimulated Zn_i^{2+} release in normal Zn^{2+}-free medium. Addition of H_2O_2 induced a marked increase in both the $[O_2^{-\bullet}]_i$ (red line; ~25-fold increase; Figures 1a, b and e) and the $[Zn^{2+}]_i$ (green line; ~45-fold increase; Figures 1a, b and f). Addition of $ONOO^-$ also induced an increase in the $[O_2^{-\bullet}]_i$ and $[Zn^{2+}]_i$ (Figures 1c, e and f).

A cell-penetrating high-affinity Zn_i^{2+} chelator, TPEN (Kd for zinc = 1.4×10^{-13} M at pH 7.0) was used to chelate release Zn_i^{2+}.[1] When it was added to the extracellular medium during the plateau of the Zn_i^{2+} increase, a rapid decrease in the $[Zn^{2+}]_i$ was seen ('post-TPEN'; Figures 1b and c), indicating that TPEN can easily penetrate the plasmalemma. Cysteine-containing reagents (GSH or *N*-acetylcysteine (NAC)) and dithiothreitol (DTT) are also suggested to be zinc chelators,[1,12] and all three reagents largely inhibited the H_2O_2- and $ONOO^-$-induced increases in the $[Zn^{2+}]_i$, whereas only NAC inhibited the $[O_2^{-\bullet}]_i$ increase (Figures 1c, e and f, Supplementary Figure S1e).

An $O_2^{-\bullet}{}_i$ chelator, MnTBAP, abolished both the H_2O_2- and the $ONOO^-$-induced increase in the $[O_2^{-\bullet}]_i$ and $[Zn^{2+}]_i$ (Figures 1e and f), indicating that the $[O_2^{-\bullet}]_i$ increase is upstream of the $[Zn^{2+}]_i$ increase. Post-TPEN inhibited the $[Zn^{2+}]_i$ increase, but not the $[O_2^{-\bullet}]_i$ increase (Figures 1b, e and f), suggesting that the Zn_i^{2+} increase caused by the oxidants also induces the $[O_2^{-\bullet}]_i$ increase and that both are prevented by pretreatment with TPEN ('pre-TPEN'; Figures 1e and f), whereas post-TPEN occurs too late to prevent the $[O_2^{-\bullet}]_i$ increase.

Positive feedback between the $[O_2^{-\bullet}]_i$ and $[Zn^{2+}]_i$ increases. Addition of either 20 μM Zn_o^{2+} to 100 mM K^+/Ca^{2+}-free EGTA medium[11] (i.e. Zn_i^{2+} supplementation) or of 1 μM Zn_o^{2+}/4 μM pyrithione to normal medium[9,10] (Figure 1d) induced similar increases in the $[O_2^{-\bullet}]_i$ and $[Zn^{2+}]_i$ (Figures 1e and f) to those produced by H_2O_2 or $ONOO^-$, and, when 10 μM Zn_o^{2+} in 40 mM K^+/Ca^{2+}-free EGTA medium was used, there was a smaller increase in the $[O_2^{-\bullet}]_i$ and $[Zn^{2+}]_i$ (~20-fold, Figures 1e and f). MnTBAP abolished 20 μM Zn_o^{2+}-induced $[O_2^{-\bullet}]_i$ increase, but not the $[Zn^{2+}]_i$ increase (dashed lines; Figures 1d, e and f), showing that the Zn_o^{2+} influx is upstream of the $[O_2^{-\bullet}]_i$ increase. These results thus suggest the existence of a positive feedback loop between the $[Zn^{2+}]_i$ and $[O_2^{-\bullet}]_i$ increases (Figure 8e).

The Zn_i^{2+} release induces TPEN-, flavonoid-, and ERK-glycogen synthase kinase-3β-sensitive myocyte apoptosis. When myocytes were exposed to H_2O_2 or $ONOO^-$, or to 10 μM Zn^{2+}/K^+ for 4 h (Figure 2), and were returned to normal medium for 24 h after 4-h exposure to these reagents (Supplementary Figure S2c), marked TPEN-sensitive cytC release (Figures 2a and b), activation of z-DEVD.fmk-/z-VAD-sensitive caspases, nuclear condensation (Figure 2d, Supplementary Figures S2c and d), and nuclear fragmentation (TUNEL (+), Supplementary Figures S2a and b) were seen. Thus, oxidative stress, nitrosative stress, or Zn_i^{2+} supplementation all stimulated TPEN-sensitive myocyte apoptosis.

We therefore examined possible molecular mechanism for the Zn_i^{2+} release-induced caspase-dependent apoptosis and found that three potent flavonoids (baicalein, luteolin, and fisetin) and commonly used antioxidants or Zn_i^{2+} chelators (MnTBAP, GSH, NAC, or DTT) all abolished the ROS/H_2O_2-, RNS/$ONOO^-$, or Zn_o^{2+}-induced cytC release (Figures 2a and b) and caspase activation at 4 h (Figures 2c and d) or 24 h (Supplementary Figure S2c). Moreover, both baicalein and U0126, which failed to inhibit the H_2O_2-, $ONOO^-$, or Zn_o^{2+}-induced ROS increase (in $O_2^{-\bullet}$ (Figure 1e); in H_2O_2 and $OH^\bullet$ (Supplementary Figure S1g)) and Zn_i^{2+} release (Figure 1f), had a marked protective effect (Figures 2b and d, Supplementary Figure S2c). Another MEK/ERK inhibitor, PD98059, also inhibited cytC release (Figure 2b).

Glycogen synthase kinase-3β (GSK-3β) was recently suggested to have an important role in cardiac I/R injury. When the reperfusion injury salvage kinase (RISK) family members PKA, PKB/Akt, PKC, and MEK-ERK are activated by pre- or post-conditioning, a common downstream protein, GSK-3β, is phosphorylated at Ser9, resulting in GSK-3β inhibition (both events occurring within 20 min of the end of conditioning), leading to the inhibition of mPTPs and the salvaging of 20–50% live myocardium.[4,5,13–16] A potent GSK-3 inhibitor, SB216763 (SB21),[4,13] had a relatively weak protective effect against H_2O_2-, $ONOO^-$-induced myocyte death (Supplementary Figure S2c), but gave better protection against 10 μM Zn^{2+}-induced cell toxicity at 4 h (Figure 2d) or 24 h (Supplementary Figure S2c) of Zn_o^{2+} exposure. Transfection of cardiomyocytes with siGSK-3β for 48 or 72 h resulted, respectively, in knockdown of GSK-3β mRNA or protein (Figure 4d). After knockdown for 72 h, siGSK-3β had a significant protective effect against Zn^{2+}/K^+-induced myocyte apoptosis (Figure 2e), but little protective effect against H_2O_2- or $ONOO^-$-induced apoptosis (2nd *versus* 3rd (+ siGSK-3β) paired bars, Figure 2e). Interestingly, TPEN or baicalein remained cardioprotective in the presence of GSK-3β knockdown ($^{\#}P < 0.05$, Figure 2e), indicating that another Zn_i^{2+}-dependent, but GSK-3β-independent pathway may exist.

Simulated I/R also induces Zn_i^{2+} release, resulting in TPEN-, ERK-, GSK-3β-, and flavonoids-sensitive myocyte apoptosis. After continuous perfusion with simulated ischemic solution for 40 min (starting at 'I' in Figures 3a and b), the perfusate was switched to oxygen-containing reperfusion solution for ~50–60 min (starting at 'R'), and a sustained increase in both the $[O_2^{-\bullet}]_i$ (upper

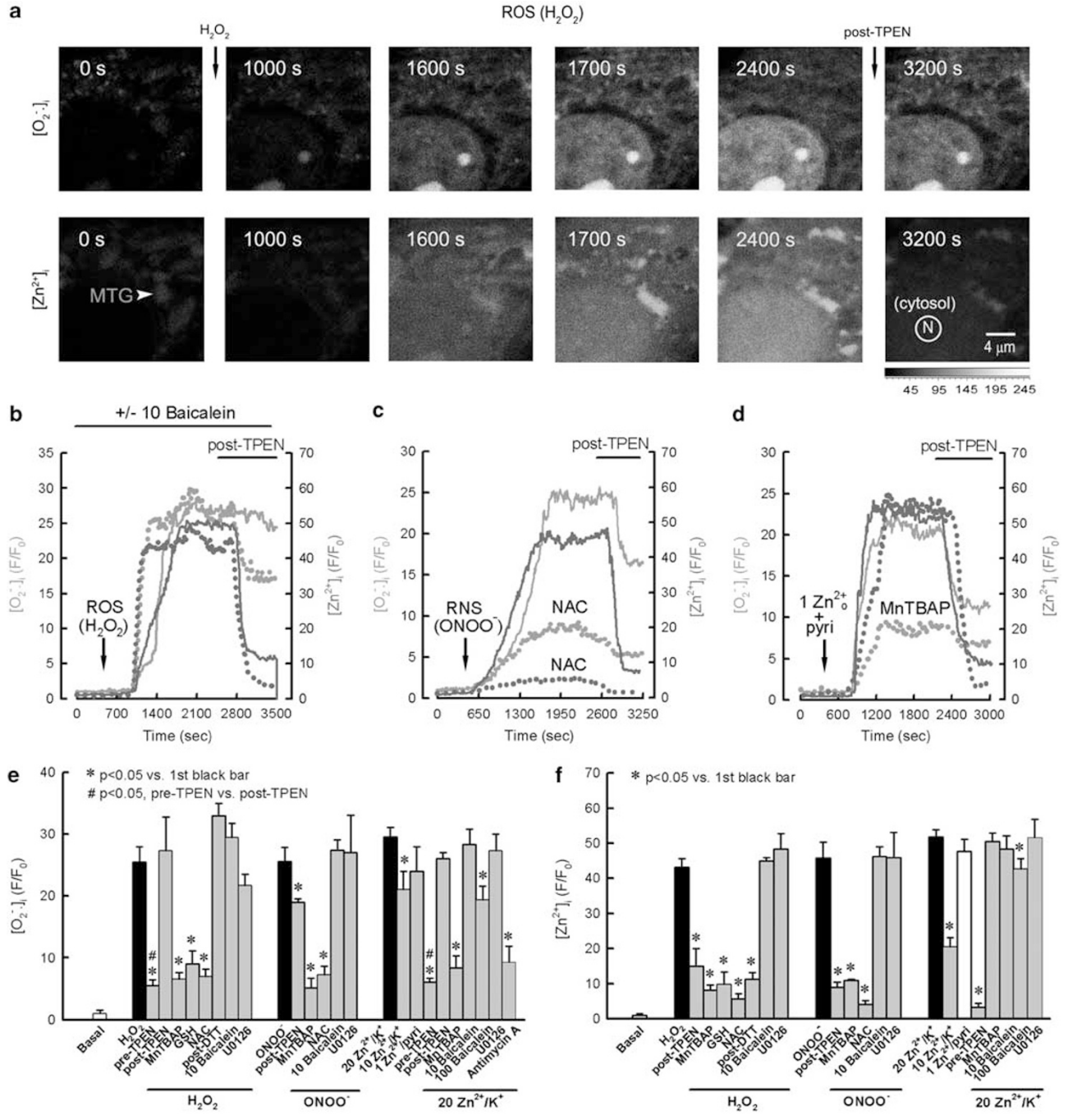

Figure 1 A sustained increase in the $[O_2^{-\bullet}]_i$ and $[Zn^{2+}]_i$ is induced in FluoZin-3 AM, MitoSox Red, and MTG triple-loaded cardiomyocytes by addition of ROS, RNS, or Zn_o^{2+}. In **b–d**, the resting level of the $[O_2^{-\bullet}]_i$ and $[Zn^{2+}]_i$ is $F/F_0 = 1$. (**a** and **b**) H_2O_2 (ROS) induces a sustained increase in the $[O_2^{-\bullet}]_i$ (upper panels in **a**, red line in **b**) and $[Zn^{2+}]_i$ (lower panels in **a**, green line in **b**). In **a**, a mitochondrion (MTG) is indicated by the arrowhead, while the region of interest (ROI) analyzed in the nuclei/cytosol ('N'), but not the mitochondria, is indicated in the last frame. The small effect of baicalein (dotted red and green lines) on the H_2O_2-induced $[O_2^{-\bullet}]_i$ and $[Zn^{2+}]_i$ increases (solid red and green lines) is shown in **b**. (**c**) $ONOO^-$ (RNS) also induces a sustained increase in the $[O_2^{-\bullet}]_i$ and $[Zn^{2+}]_i$. Pretreatment with NAC markedly inhibits both increases. (**d**) 1 μM Zn_o^{2+}/4 μM pyrithione causes a sustained increase in the $[O_2^{-\bullet}]_i$ and $[Zn^{2+}]_i$ ($\sim$45-fold, solid lines). Note that MnTBAP inhibits the Zn_o^{2+}-induced $[O_2^{-\bullet}]_i$ increase (dotted red line), but not the TPEN-sensitive $[Zn^{2+}]_i$ increase (dotted green line). The $[Zn^{2+}]_i$ increase, but not the $[O_2^{-\bullet}]_i$ increase, is completely reversed by addition of TPEN at the end of the experiment (post-TPEN, **b**, **c** and **d**). (**e** and **f**) Summarized data. The vehicle controls contained 0.1% ethanol. A mitochondrial complex-III inhibitor, antimycin A, markedly inhibited the Zn_o^{2+}/K^+-induced $[O_2^{-\bullet}]_i$ increase (**e**), indicating that the $O_2^{-\bullet}$ production may be induced by an increase in $[Zn^{2+}]_{mito}$ (cf. Supplementary Figure S1b), resulting in complex III activation (*$P<0.05$; $n=6$–9/group). For the concentrations of all reagents used, see the Supplemental Methods. The color reproduction of this figure is available at the *Cell Death and Differention* journal online

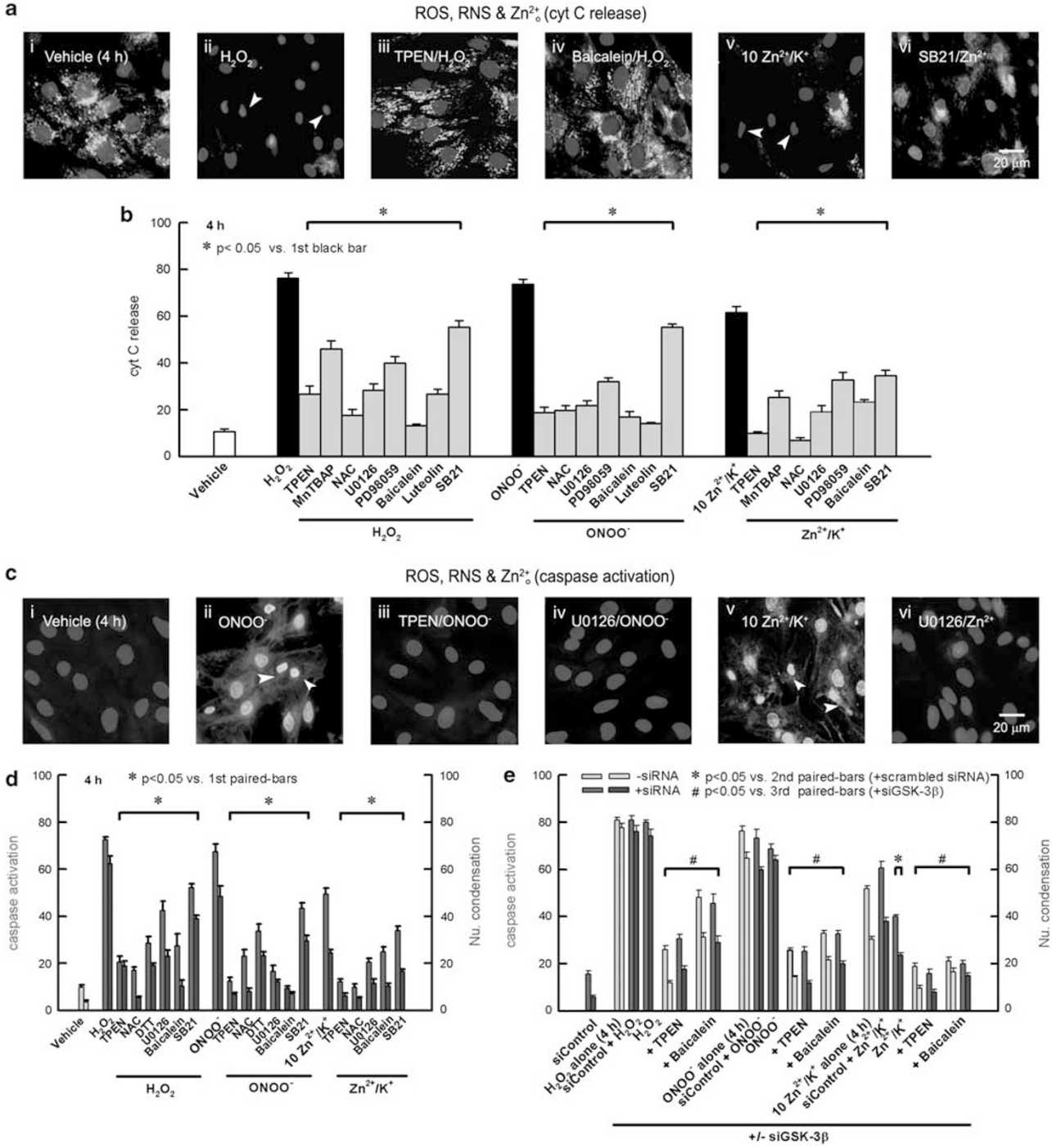

Figure 2 Exposure to ROS, RNS, or Zn^{2+}_o causes TPEN-, NAC-, DTT-, U0126-, and flavonoid-sensitive cytC release and caspase-dependent nuclear condensation. (**a** and **b**) CytC release. Anti-cytC antibody (green fluorescence within intact mitochondria, see **a**i: vehicle) was used to detect cytC release (arrowheads in **a**ii) after addition of H_2O_2, $ONOO^-$, or 10 *i*M Zn^{2+}/K^+ for 4 h with or without inhibitors (**b**). (**c** and **d**) After addition of H_2O_2, $ONOO^-$, or 10 *i*M Zn^{2+}/K^+ for 4 h with or without inhibitors, caspase activation (green in **c**, arrowheads in **c**ii) and nuclear condensation (condensed light blue nuclei, **c**ii) were measured. (**e**) After transfection with siGSK-3ß or scrambled siRNA (marked 'siControl') for 72 h, cells were treated for 4 h with or without inhibitors, then caspase activation and nuclear condensation were measured. In **b**, **d**, and **e**, $n = 5$–10/group. The color reproduction of this figure is available at the *Cell Death and Differention* journal online

panels) and $[Zn^{2+}]_i$ (lower panels, Figures 3a and b) was seen, which was similar in size to the $[O_2^{-\bullet}]_i$ and $[Zn^{2+}]_i$ increases (~20-fold) caused by exposure to 10 μM Zn^{2+}. Again, post-TPEN largely reversed the reperfusion-induced $[Zn^{2+}]_i$ overload, but not the $[O_2^{-\bullet}]_i$ overload (Figures 3b, e and f).

Pretreatment with MnTBAP also markedly inhibited the reperfusion-induced $[O_2^{-\bullet}]_i$ and $[Zn^{2+}]_i$ overloads (Figures 3e

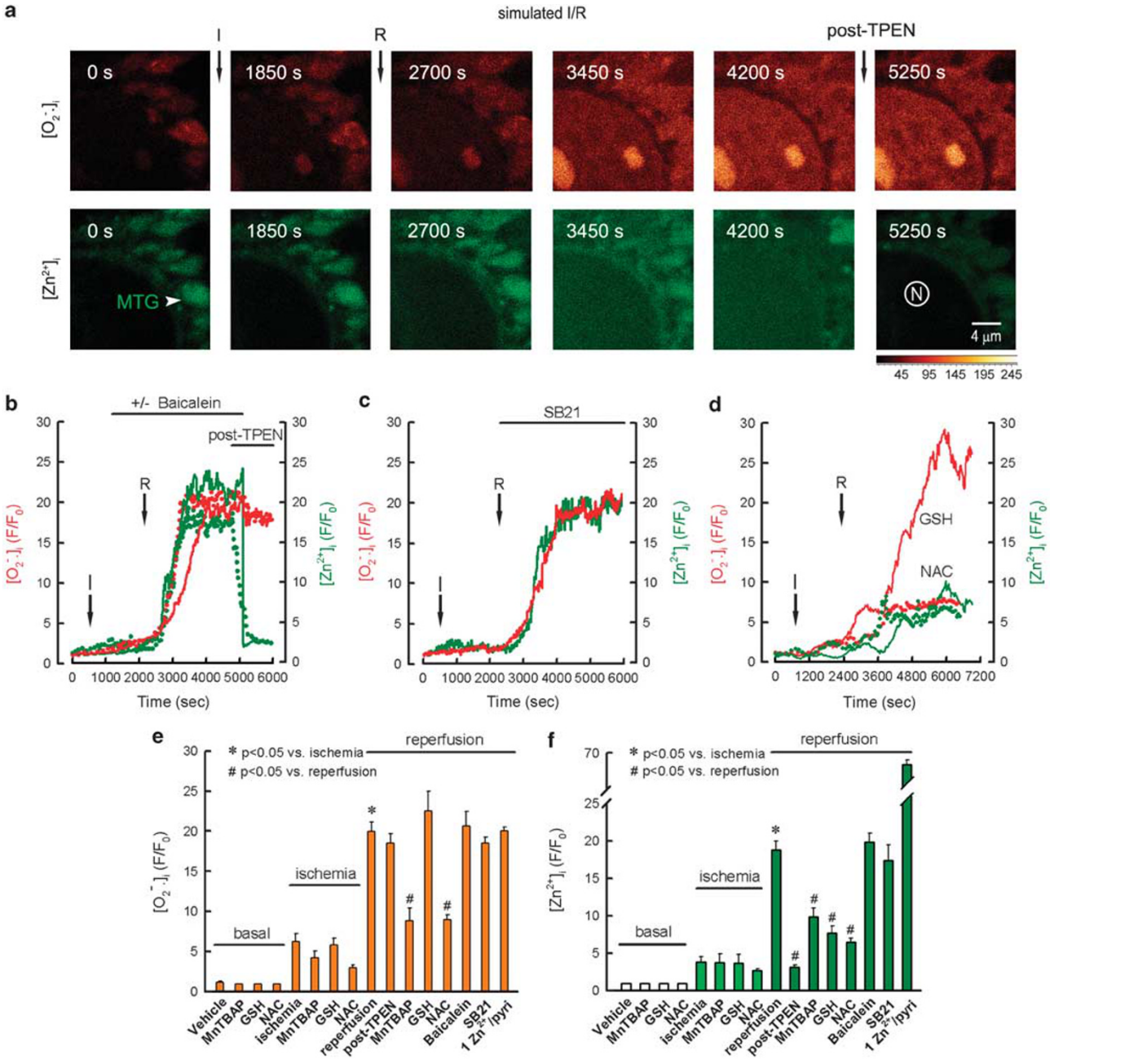

Figure 3 Simulated I/R also induces increases in the $[O_2^{-\bullet}]_i$ and $[Zn^{2+}]_i$. (**a** and **b**) Simulated ischemia ('I') has little effect on the $[O_2^{-\bullet}]_i$ and $[Zn^{2+}]_i$, while reperfusion ('R') induces a similar increase in the $[O_2^{-\bullet}]_i$ and $[Zn^{2+}]_i$ (~20-fold) to that induced by 10 μM Zn^{2+}/40 mM K^+ (cf. Figures 1e and f). The reperfusion-induced $[O_2^{-\bullet}]_i$ increase (solid or dashed red line) is not inhibited by baicalein (dashed red line in **b**) or post-treatment with TPEN (solid and dashed red lines in **b**), by SB21 (solid red line in **c**), or by GSH (solid red line in **d**), but is inhibited by NAC (dashed red line in **d**). The $[Zn^{2+}]_i$ increase (solid and dashed green lines) is inhibited by post-treatment with TPEN (**b**), GSH (solid green line in **d**), or NAC (dashed green line in **d**), but not by baicalein (dashed green line in **b**) or SB21 (**c**). (**e** and **f**) Summarized data. The data are the mean ± SEM; $n = 6$–8/group

and f), again, indicating that the $[O_2^{-\bullet}]_i$ overload is upstream of the Zn_i^{2+} release. Pretreatment with GSH markedly inhibited the $[Zn^{2+}]_i$ overload, but not the $[O_2^{-\bullet}]_i$ overload, while NAC inhibited both overloads (Figure 3d). As GSH and NAC are both cysteine-rich reagents, the inhibitory effect on the $[Zn^{2+}]_i$ increase, but not the $[O_2^{-\bullet}]_i$ overload, was possibly due to acceleration of Zn^{2+} re-uptake by cysteines, as shown in an *in vitro* study.[1] In contrast, when a mixture of 1 μM Zn^{2+}/4 μM pyrithione was added for ~30 min at the start of reperfusion, $[O_2^{-\bullet}]_i$ overload and a more marked increase in the $[Zn^{2+}]_i$ (>65-fold) were seen (Figures 3e and f), indicating additional Zn_o^{2+} influx when Zn_o^{2+}/pyrithione was applied.

We next investigated whether the TPEN-/NAC-/GSH-sensitive Zn_i^{2+} increase/release (Figures 3d and f) had an effect on cell survival after simulated I/R exposure. The experiments shown in Figures 4a and b (caspase activation

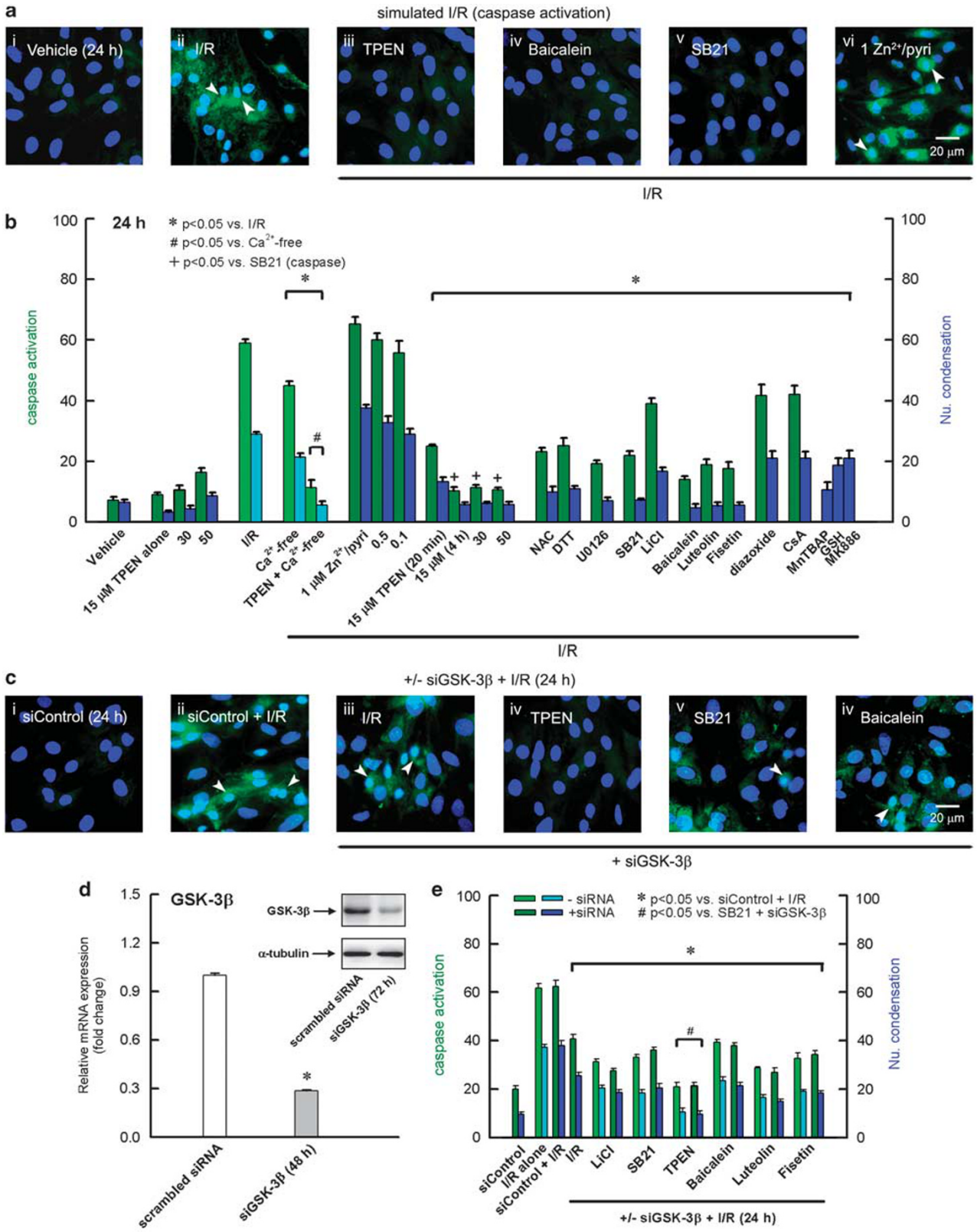

Figure 4 TPEN, NAC, DTT, U0126, flavonoids, or GSK-3β inhibitors abolish simulated I/R-induced apoptosis. (**a** and **b**) If not otherwise specified, the inhibitor was only present during the 4-h reperfusion. Caspase activation (green and arrowheads) and nuclear condensation (light blue and condensed nuclei) are shown in **a**ii. (**c**–**e**) Myocytes were transfected with 100 nM siGSK-3β for 48 or 72 h, respectively, resulting in knockdown of GSK-3β mRNA or protein (**d** and inset). At 72 h after transfection with siRNA or control scrambled siRNA, inhibitors were added for 4 h during the reperfusion period. (**e**) Summarized data; $n = 7$–10/group

and nuclear condensation) and supplemental Figures S2a and b (TUNEL test) were performed as follows: after ischemia for 40 min, followed by reperfusion for 4 h, myocytes were returned to normal medium without inhibitors for 24 h, then were examined for apoptotic markers. Compared with I/R alone ('I/R', Figure 4b), the presence of 15 μM TPEN at the start of reperfusion for only $\sim$20 min ('TPEN (20 min)') markedly inhibited I/R injury at 24 h after TPEN removal, suggesting that the reperfusion-induced initial Zn_i^{2+} release (Figure 3b) is important in I/R injury. When 15–50 μM TPEN was present throughout the 4 h reperfusion period, surprisingly, it almost completely abolished apoptosis at 24 h (Figures 4a and b, Supplementary Figures S2a and b). In contrast, when Zn^{2+}/pyrithione was added for only $\sim$20 min at the beginning of reperfusion, it had little protective effect for both cardiomyocytes and H9c2 cells (Figures 4a and b; Supplementary Figures S2a and b). Inclusion of any of three potent flavonoids or U0126 for 4 h in the reperfusion solution again had a marked cardioprotective effect for at least 24 h (Figures 4a and b; Supplementary Figures S2a and b), while Ca^{2+}-free medium (inhibition of I/R-induced Ca_i^{2+} overload),[5] CsA (an mPTP inhibitor),[13] diazoxide (an mK_{ATP} opener),[7] or MK886 (a selective 5-LOX inhibitor[8]) were less protective (Figures 4a and b).

We confirmed that GSK-3 inhibitors (SB21 or LiCl) and antioxidants exhibited significant cardioprotection in myocytes (Figure 4b). When GSK-3β was selectively knocked down by transfection with siGSK-3β (Figure 4d), significant protection against I/R injury for 24 h was seen (Figures 4c and e, 4th *versus* 3rd groups of darker paired bars). TPEN treatment with or without protein knockdown was again more cardioprotective than SB21 treatment ($^{\#}P<0.05$; Figure 4e), while LiCl, baicalein, or fisetin had a similar protective effect to SB21.

The Zn_i^{2+} release may also be involved in I/R injury in adult-rat hearts. Figure 5 shows that, when 15, 30, and 50 μM TPEN was used, 15 μM TPEN was the most effective, with a reduction in global infarct area of $\sim$65%. The protective effect of baicalein was similar to that of the GSK-3 inhibitor LiCl. Compared with LiCl alone, co-addition of TPEN resulted in a small, but significant, additional protective effect ($11.5\pm0.4\%$, $^{\#}P<0.05$), again suggesting that another Zn_i^{2+}-dependent, but GSK-3β-independent pathway may exist.

The ERK-dependent GSK-3β–p53 pathway and Noxa–myeloid cell leukemia signaling are both involved in the Zn_i^{2+} increase-induced myocyte death. In neurons, it has been suggested that the Zn_i^{2+} release activates the ERK–LOX–ROS cascade, resulting in neuronal apoptosis.[8] In Supplementary Figures S4 and S5, we have ruled out a possible role for lipoxygenase, nuclear factor κB (NFκB), or hypoxia-inducible factor-1 (HIF1α) on the Zn_i^{2+} increase-induced myocyte death. As U0126 and TPEN were both cardioprotective and also there is little information whether the I/R-induced Zn_i^{2+} increase activates both ERK and GSK-3β, resulting in myocyte apoptosis, we tested this hypothesis.

In cardiomyocytes (Figure 6A) or H9c2 cells (Supplementary Figure S3b), Zn_i^{2+} supplementation caused an early

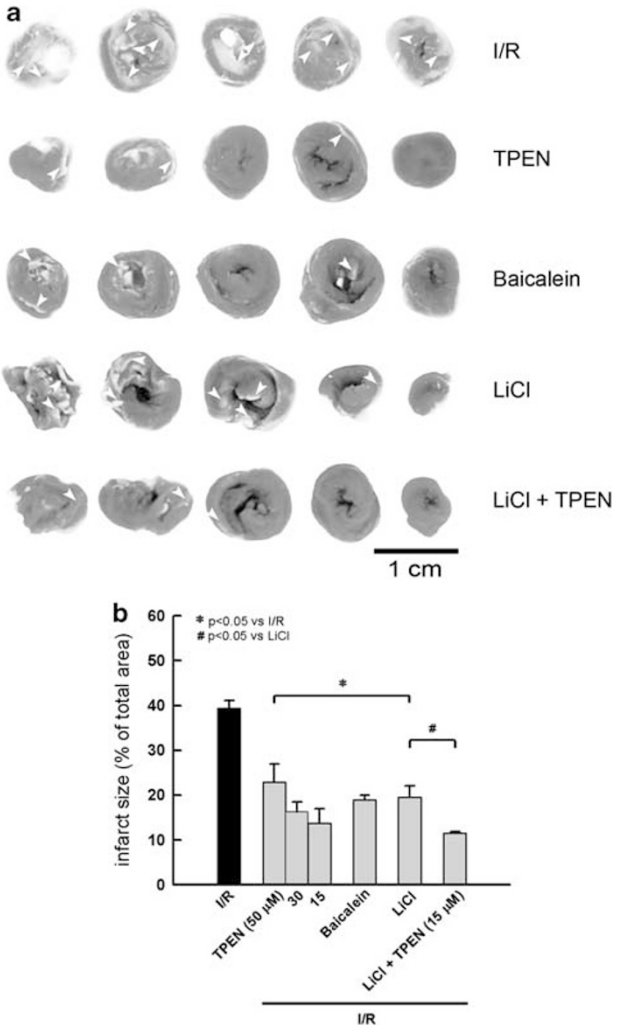

Figure 5 Both TPEN and baicalein have a marked protective effect in adult-rat hearts. (**a**) After 30 min of ischemia, TPEN or baicalein was added to the reperfusion solution for 2 h. The vehicle was 0.1% ethanol. In the group receiving LiCl (a GSK-3 inhibitor), 10 mM NaCl in the reperfusion solution was replaced with 10 mM LiCl. (**b**) Compared with the LiCl group, the mixture of LiCl and TPEN provides extra protection ($^{\#}P<0.05$). Infarct size was determined as the percentage of white tissue in the total cross-section area (arrowheads in **a**)

increase in p-ERK1/2 levels at 2 h or 20 min, respectively, and p-ERK1/2 levels remained high for 2–5 h thereafter. This persistent increase in p-ERK1/2 levels was abolished by TPEN or U0126, but not by baicalein or MnTBAP (Figures 6a and b; Supplementary Figures S3a and b).

In non-cardiac cells, it has been suggested that GSK-3β dephosphorylation at Ser9 and/or its phosphorylation at Tyr216 increases the activity of the enzyme.[17,18] In adult-rat hearts, however, phosphorylation of Tyr216 in GSK-3β does not change after 5 min of reperfusion.[14] After short Zn_i^{2+} supplementation of cardiomyocytes for 2 h (Figure 6A) or of H9c2 cells for 20 min (Supplementary Figure S3b), a simultaneous increase in p-ERK1/2 and p-Ser9 GSK-3β (GSK-3β inhibition) was seen. However, when the p-ERK1/2 increase lasted for 3–5 h, dephosphorylation of p-Ser9 and phosphorylation of p-Try216 on GSK-3β were seen (Figure 6A, Supplementary Figure S3b), indicating that a

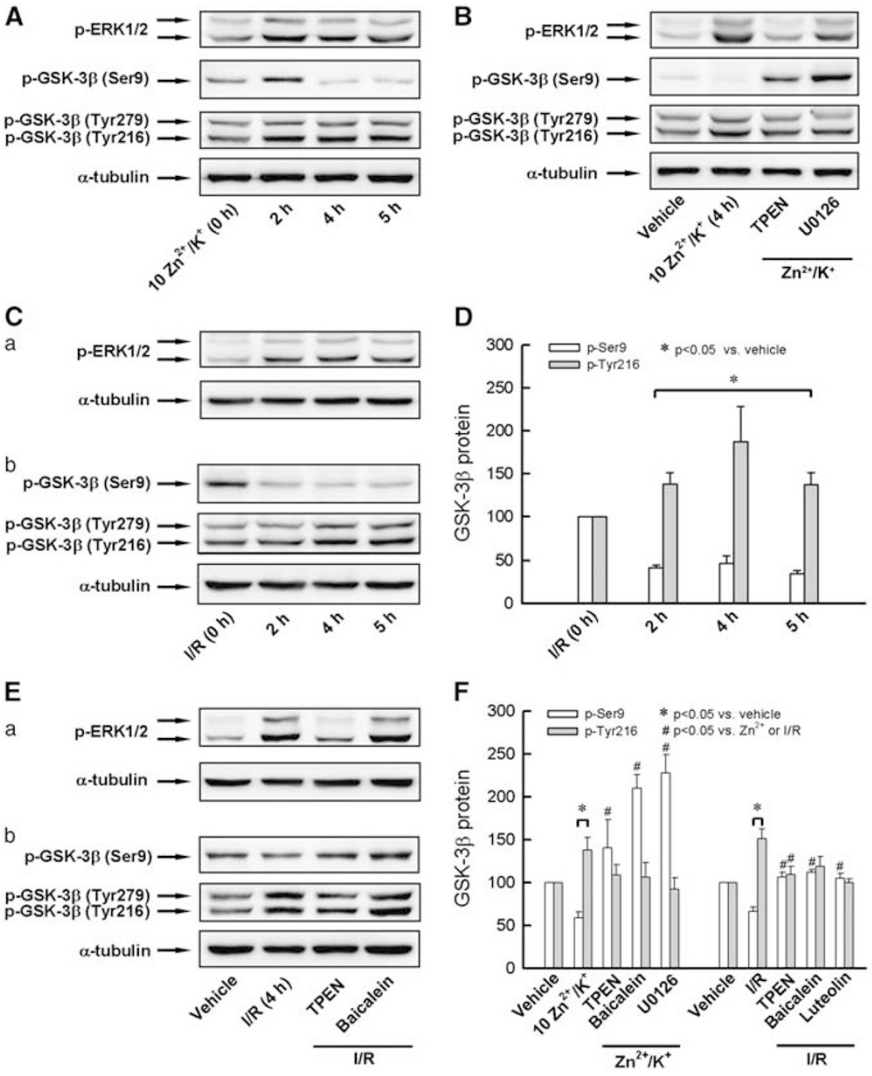

Figure 6 Inhibitory effects of TPEN, U0126, or flavonoids on the I/R- and Zn_o^{2+}-induced activation of ERK1/2 and GSK-3β in cardiomyocytes. (**A**) Western blot showing the time course of the effect of Zn_i^{2+} supplementation on ERK1/2 and GSK-3β activity. (**B**) TPEN, U0126, or baicalein inhibits the 10 μM Zn^{2+}/K^+-induced activation of ERK1/2 and GSK-3β (i.e. p-Ser9 decrease and p-Try216 increase) at 4 h of treatment. (**C** and **D**) Time course of the simulated I/R-induced activation of ERK1/2 (**C**a) and GSK-3β (**C**b) and the summarized data (**D**). (**E**) TPEN and baicalein abolish the I/R-induced activation of p-ERK1/2 (**E**a) and GSK-3β (**E**b) at 4 h of reperfusion. (**F**) Summarized data for the phosphorylation of GSK-3β. Data are taken from **B** and **E**. In **D** and **F**, $n = 5$–8/group

long-lasting $[Zn^{2+}]_i$ increase unexpectedly activated both ERK1/2 and GSK-3β. Moreover, TPEN (Figure 6B, Supplementary Figure S3b), U0126 (Figure 6B), or baicalein (Figure 6F) largely inhibited GSK-3β activation in cardiomyocytes by increasing p-Ser9 GSK-3β levels, but there was no statistically significant reduction in p-Tyr216 GSK-3β levels (Figure 6F, Zn_o^{2+} *versus* inhibitors, $^{\#}P < 0.05$).

Using I/R in cardiomyocytes, a similar response of a persistent p-ERK1/2 increase (Figure 6Ca) and dephosphorylation of Ser9 and phosphorylation of Tyr216 on GSK-3β (Figures 6Cb–D) was seen during 2–5 h of reperfusion. TPEN abolished the I/R-induced persistent p-ERK1/2 increase (Figure 6Ea) and reversed the Ser9 dephosphorylation and Tyr216 phosphorylation (Figures 6Eb–F). Baicalein (Figures 6Eb–F) or leuteolin (data not shown) reversed the dephosphorylation of p-Ser9. Thus, the target of the flavonoids is probably a protein downstream of ERK1/2, for example, GSK-3β (Figure 8e). All three inhibitors reduced the mean p-Tyr216 GSK-3β value, but only TPEN had a significant effect (Figure 6F), as the intensity of the p-Tyr216 band varied between batches of primary myocytes.

Figure 7a shows confocal images demonstrating that I/R treatment for 4 h induced an increase in p-Tyr216 GSK-3β levels in myocyte nuclei (arrow in Aii; $26.7 \pm 1.8\%$, $n = 6$) and that this increase was abolished by TPEN ($3.5 \pm 0.6\%$, $n = 6$) or baicalein ($8.6 \pm 0.6\%$, $n = 6$). A similar inhibitory effect of TPEN or U0126 (both $< 5\%$, $n = 5$, Figure 7biii) on Zn^{2+}/K^+-induced p-Tyr216 GSK-3β translocation in myocyte nuclei was also seen (arrow in Figure 7bii; 23.6(3.8%, $n = 5$). After I/R exposure for 4 h, followed by a return to normal medium for 24 h (Figure 7cii), an increase in co-expression of GSK-3β (green) and p53, a GSK-3β substrate protein (red), was seen

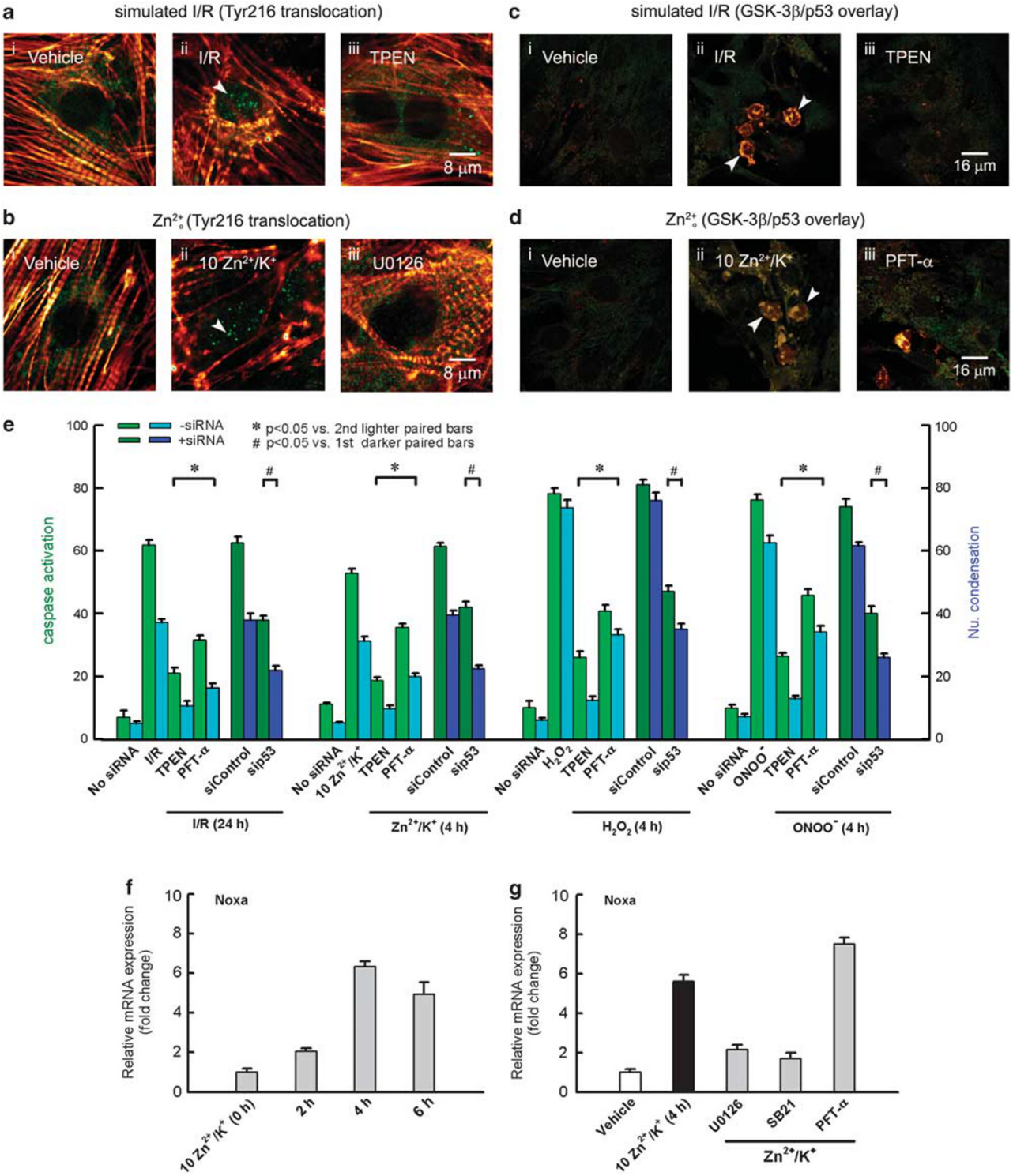

Figure 7 Simultaneous activation of GSK-3β and p53 and an increase in Noxa expression are involved in Zn_i^{2+} increase-induced myocyte death. (**a**–**d**) Representative confocal microscopic images of p-Tyr216 GSK-3β translocation into the myocyte nucleus (**a** and **b**) and GSK-3β–p53 activation (**c** and **d**). TPEN, U0126, baicalein, or PFT-α (a p53 inhibitor) inhibit the increase in p-Tyr216 in myocyte nuclei (punctate green fluorescence, arrowhead in **a** and **b**) or the colocalization of GSK-3β (green) and p53 (red) in nuclei (yellow, arrowhead in **c** and **d**). (**e**) Treatment with either PFT-α or sip53 is protective against I/R-, 10 μM Zn^{2+}/K^+-, H_2O_2-, or $ONOO^-$-induced myocyte death. $n = 4$–8/group. (**f**) Time course of the induction of an increase in Noxa mRNA caused by 10 μM Zn^{2+}/K^+ exposure measured by quantitative real-time PCR (qPCR). (**g**) U0126 or SB21, but not PFT-α, abolishes the increase in Noxa expression at 4 h of Zn_i^{2+} supplementation

in nuclei (overlay/yellow: I/R: 25.5 ± 3.1%, $n=6$), and this effect was again inhibited by TPEN (5.1 ± 2.4%, $n=5$, Figure 7ciii) or baicalein (7.3 ± 2.6%, $n=4$). A similar inhibitory effect of TPEN (3.4 ± 1.7%, $n=4$) or baicalein (11.3 ± 2.6%, $n=4$) was also seen after Zn^{2+}/K^+ exposure for 4 h and return to normal medium for 24 h (36.3 ± 2.5%, $n=9$, Figure 7dii).

Pifithrin-α PFT-α inhibits the p53-dependent transactivation of p53-responsive genes and reversibly blocks p53-mediated apoptosis.[19] Pretreatment with PFT-α largely inhibited the Zn^{2+}/K^+-induced p53 expression ($P<0.05$; 55.0 ± 2.7% *versus* 25.8 ± 1.9%, $n=5$) and GSK-3β/p53 co-expression in nuclei ($P<0.05$; 36.3 ± 2.5% *versus* 19 ± 1.5%, $n=9$ and 5, respectively, Figure 7diii), but had little effect on the expression of GSK-3β *per se* ($P>0.05$; 68.5 ± 2.7% *versus* 60 ± 4.1%, $n=5$). PFT-α also significantly inhibited TPEN-sensitive I/R-, H_2O_2-, $ONOO^-$-, or Zn^{2+}/K^+-induced myocyte death ($^*P<0.05$, 2nd *versus* 4th groups of lighter paired bars (−siRNA) in Figure 7e). Moreover, silencing of p53 expression by sip53 transfection also provided significant cardioprotection ($^\#P<0.05$, 1st *versus* 2nd groups of darker paired bars (+siRNA) in Figure 7e). Taken together, these data suggest that activation of ERK-dependent GSK-3β–p53 signaling is involved in the Zn_i^{2+} increase-induced myocyte death.

It has been suggested that the apoptotic protein Noxa is a transcriptional target of p53.[20] An anti-apoptotic Bcl-2 family protein, myeloid cell leukemia-1 (Mcl-1), has a high affinity for Noxa and binds to it, thus decreasing its apoptotic activity.[20,21] Moreover, activation of the Noxa–Mcl-1 pathway was recently implicated in non-cardiac cell death caused by DNA-damaging agents, including H_2O_2 and cisplatin.[21,22] Figures 7f and g show that exposure to Zn^{2+}/K^+ resulted in a transient increase in Noxa mRNA levels, which peaked at 4 h. The I/R or H_2O_2 exposure also induced a marked increase in Noxa mRNA levels (Supplementary Figures S3c and d). Interestingly, this increase was largely inhibited by U0126 or SB21, but not by PFT-α (Figure 7g, Supplementary Figure S3c), suggesting that the Zn_i^{2+} increase induces ERK-/GSK-3-dependent, but p53-independent, Noxa expression (Figure 8e). Furthermore, TPEN, U0126, SB21 (Figures 8b and c), or baicalein (Supplementary Figure S3f) simultaneously abolished the I/R- or Zn_i^{2+} supplement-induced increase in Noxa protein levels, and decrease in Mcl-1 protein levels. Moreover, the Zn_i^{2+} supplementation-induced Mcl-1 decrease was inhibited by a proteosomal inhibitor MG132 (Figure 8a), indicating that the decrease is due to an increase in proteosomal degradation (Figure 8e). The cell death assay also demonstrated that silencing of Noxa expression resulted in significant cardioprotection against I/R-, H_2O_2-, $ONOO^-$-, or Zn^{2+}/K^+-induced apoptosis (Figure 8d), while knockdown of Mcl-1 did not. Interestingly, an additional small protective effect was consistently observed when SB21 or PFT-α was present after silencing Noxa expression for 65–72 h (Figure 8d), indicating that both the Noxa–Mcl-1 and GSK-3β–p53 axes, which are downstream of the activated ERK1/2, are involved in the myocyte death (Figure 8e). We did not perform double knockdown experiments in Figure 8d, as cardiomyocytes transfected with both siRNAs were not healthy after 65–72 h transfection. SB21 or siGSK-3β had only a small, or no, protective effect against H_2O_2-/$ONOO^-$-induced cell death (Figures 2d and e, Supplementary Figure S2c); the reason for this is not known, but the larger Zn_i^{2+} release caused by exposure to H_2O_2- or $ONOO^-$ may activate ERK–p53–Noxa-dependent, but GSK-3β-independent, signaling (Figures 7e, 8d and e).

Discussion

Oxidative stress and nitrosative stress are both considered as major causes of cardiac I/R injury.[3–5] This study provides two novel results: (i) using time-lapse confocal microscopy and high-affinity Zn^{2+}-selective fluorescent probes, I/R, ROS, and RNS were found to cause marked endogenous Zn_i^{2+} release, which increased ERK1/2 activity, resulting in the activation of both GSK-3β–p53 and Noxa–Mcl-1 signaling and myocyte death (Figure 8e); and (ii) short exposure to TPEN or flavonoids at the start of reperfusion may have beneficial therapeutic potential.

When myocytes were treated with simulated I/R, ROS, or RNS, all caused significant TPEN-sensitive Zn_i^{2+} release, with positive feedback between the $[Zn^{2+}]_i$ and $[O_2^{-\bullet}]_i$ increases (Figures 1d and 8e). At least two independent Zn_i^{2+} pools were found to be located in the cytosolic and mitochondrial compartments, respectively, and the released Zn^{2+} translocated between the two compartments (Supplementary Figures S1c and d), as shown previously in neurons.[11]

When TPEN was applied for only 20 min at the beginning of the 4-h reperfusion, there was a marked protective effect that lasted for at least 24 h (Figure 4b, Supplementary Figure S2b), suggesting that the initial Zn_i^{2+} release, evoked by a burst of $O_2^{-\bullet}{}_i$ at the beginning of reperfusion (Figure 3b), is an important early death signal for the I/R injury seen at 24 h. When TPEN was applied throughout the 4-h reperfusion period, it provided more cardioprotection than other treatments, including GSK-3 inhibition, flavonoids, Ca^{2+}-free medium, CsA, or diazoxide (Figure 4b). TPEN also markedly abolished the Zn_i^{2+}-dependent H_2O_2- or $ONOO^-$-induced apoptosis. Moreover, three membrane-permeating thiols (GSH, NAC. and DTT), which prevent oxidation of protein sulfhydryl groups,[1,12] all abolished the marked Zn_i^{2+} release, but only NAC inhibited the $[O_2^{-\bullet}]_i$ increase. As these reagents were all cardioprotective, again, this indicates that NAC-/GSH-/DTT-induced intracellular Zn^{2+} chelation may prevent the myocyte death. In contrast, when a Zn^{2+}/pyrithione mixture was added to the reperfusion solution for ~30 min, a much larger $[Zn^{2+}]_i$ increase was seen, and marked apoptosis was seen at 24 h after its addition to the reperfusion solution for only 20 min (Figure 4b, Supplementary Figure S2b).

There is mounting evidence in adult-rat hearts that within 20–30 min of the end of pre- or post-conditioning, RISK family members are activated, resulting in phosphorylation of GSK-3β at Ser9 (i.e. GSK-3β inhibition), which protects the adult-rat heart from I/R injury for 2–4 h.[4,13–16] This study showed a link between the Zn_i^{2+} release/increase and the activation of GSK-3β, resulting in myocyte apoptosis. We observed an early increase in p-Ser9 GSK-3β levels after Zn_i^{2+} supplementation of cardiomyocytes for 2 h or of H9c2 cells for 20 min, in agreement with the results of Xu and co-workers[23,24] in H9c2 cells that Zn_i^{2+} supplementation for

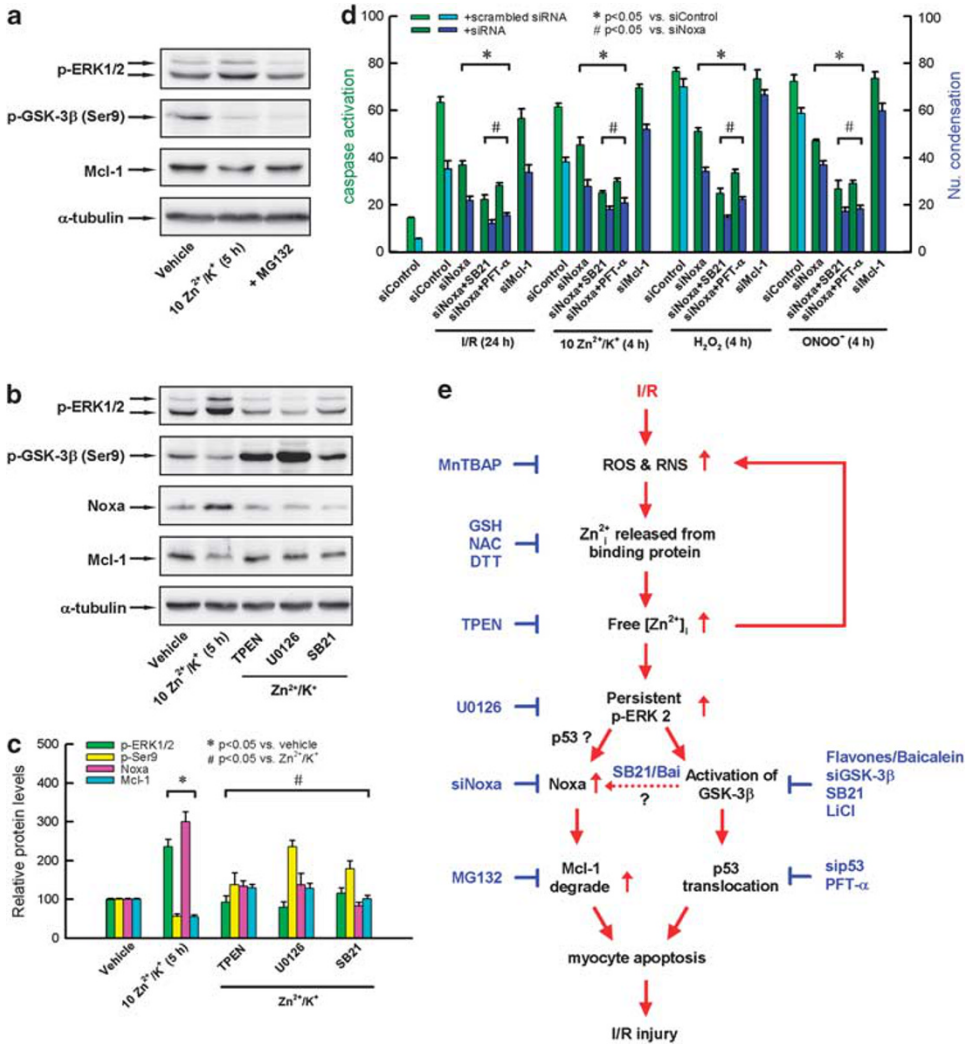

Figure 8 (**a**–**c**) The Zn_i^{2+} increase induces both Noxa protein expression and MG132-sensitive Mcl-1 protein degradation, and these effects are blocked by pretreatment with TPEN, U0126, or SB21 (**a** and **b**). Zn_i^{2+} supplementation induces p-ERK activation and GSK-3β dephosphorylation/inhibition (**b** and **c**). (**d**) Noxa expression is involved in the I/R-, 10 μM Zn^{2+}/K^+-, H_2O_2-, or $ONOO^-$-induced myocyte death. Silencing of Noxa expression for 65–72 h (marked siNoxa) induces significant protection against myocyte apoptosis ($^*P<0.05$). SB21 or PFT-α provides additional myocyte protection after silencing of Noxa protein ($^{\#}P<0.05$). (**e**) Schematic diagram showing that oxidative stress and nitrosative stress both induce Zn_i^{2+} release, resulting in TPEN- and flavonoid-sensitive myocyte apoptosis. There is a positive feedback loop between the $[Zn^{2+}]_i$ and $[O_2^{-\bullet}]_i$ increases. Two independent pathways downstream of the Zn_i^{2+} increase-induced ERK activation are probably involved in the myocyte death, although other mechanisms are not ruled out (see Discussion). The flat-tipped blue arrows represent inhibition, while the red arrows represent stimulation or an increase

20 min induces phosphorylation at Ser9. However, we found that this increase disappeared after 3–5 h of Zn_i^{2+} supplementation and was followed by full activation of GSK-3β by dephosphorylation of Ser9 and phosphorylation/translocation of Tyr216 (Figure 6A, Supplementary Figure S3b), resulting in the accumulation of both GSK-3β and PFT-α-sensitive p53 in myocyte nuclei. TPEN, U0126, or flavonoids abolished the I/R- or Zn_i^{2+} supplementation-induced GSK-3β activation and the accumulation of GSK-3β and p53 in the nucleus (Figures 7A–D). Moreover, treatment with PFT-α or silencing of p53 expression significantly protected myocytes from TPEN-sensitive I/R-, H_2O_2-, $ONOO^-$-, or Zn^{2+}/K^+-induced cell death (Figure 7e). These data indicate that the GSK-3β–p53 pathway may be involved in the myocyte death. As short exposure to 0.1–10 μM Zn_o^{2+} alone or its addition to the reperfusion solution for 20 min both induced significant TPEN-/NAC-/DTT-sensitive apoptosis at 24 h (Figure 4b, Supplementary Figure S2b), we conclude that Zn_i^{2+} supplementation-induced early phosphorylation at Ser9 is not necessarily cardioprotective and may induce cytotoxicity after return to normal medium for 4 or 24 h. In support of the above conclusions, Tyr216 phosphorylation is required for nuclear GSK-3β accumulation in neurons and fibroblasts,[17,18] as mutation of Tyr216 to phenylalanine or its dephosphorylation results in less GSK-3β being found in nuclei.[17] In addition, the increase in GSK-3β in the nucleus stabilizes one of its substrate proteins, p53, which forms a complex and promotes neuronal apoptosis.[18,25] Thus, the modulation of Tyr216 GSK-3β may be as important as that of Ser9 in myocyte apoptosis.

Early activation of MEK1/2–ERK1/2 signaling is a protective upstream signal that induces phosphorylation of GSK-3β Ser9, resulting in cardioprotection.[5,16] However, a sustained p-ERK1/2 increase has been demonstrated to induce cell apoptosis in many non-cardiac cells.[21,22,26] We found that both TPEN and U0126 inhibited not only the persistent p-ERK1/2 increase but also reversed Ser9 dephosphorylation and Tyr216 phosphorylation, resulting in an inhibition of the I/R- and Zn_i^{2+} supplement-induced GSK-3β activation (Figure 6). As TPEN, U0126, and PD98059 were all cardioprotective, one possible explanation is that the Zn_i^{2+} increase-stimulated persistent ERK1/2 activation, resulting in fully activated GSK-3β (e.g. at Try216), has a role in the myocyte apoptosis (Figure 8e). However, it is currently unclear how zinc causes ERK activation/phosphorylation. It has been suggested that, in non-cardiac cells, Ras and/or Raf might be the upstream kinases causing zinc-induced ERK phosphorylation, as treatment with a Raf-1 kinase inhibitor or infection with recombinant virus expressing dominant-negative mutants of MEK both attenuate Zn^{2+}-dependent ERK phosphorylation.[8,27] However, further studies are required as regards cardiac I/R injury.

The Noxa–Mcl-1 pathway was recently implicated in cell death caused by DNA-damaging agents, for example, H_2O_2 or cisplatin.[21,22] This study showed that TPEN or U0126 was consistently more protective against H_2O_2- or $ONOO^-$-induced myocyte apoptosis than SB21 or siGSK-3β, indicating that a GSK-3β-insensitive mechanism is involved. As we found that (i) U0126 abolished the I/R or Zn_i^{2+} supplementation-induced Noxa mRNA/protein expression and MG132-sensitive Mcl-1 degradation (Figures 7g, 8b and c, Supplementary Figure S3c), and (ii) significant myocyte protection was seen after silencing of Noxa expression, but not of Mcl-1 expression (Figure 8d), the ERK-dependent Noxa–Mcl-1 pathway is also involved in myocyte death (Figure 8e). Furthermore, activation of GSK-3β–p53 and Noxa–Mcl-1 signaling are two independent pathways downstream of the Zn^{2+}-dependent ERK1/2 activation (Figure 8e), as PFT-α had little effect on Noxa mRNA expression and additional cardioprotection by either SB21 or PFT-α was observed after knockdown of Noxa (Figures 7g and 8d).

There is evidence that Mcl-1 contains an evolutionarily conserved GSK-3 site,[28] and activated GSK-3β has been suggested to physically associate with, and phosphorylate, Mcl-1 at Ser159, which then facilitates the ubiquitination and degradation of p-Mcl-1 and contributes to GSK-3β-induced apoptosis.[28,29] Surprisingly, we found that baicalein or SB21 had a similar inhibitory effect against the Zn_i^{2+}-dependent GSK-3β activation and both abolished the increase in Noxa mRNA/protein and the decrease in Mcl-1 protein (Figures 6F, 7g, 8b and c, Supplementary Figures S3c and f). The cell death assay showed that knockdown of the apoptotic protein Noxa resulted in cardioprotection, while knockdown of the anti-apoptotic protein Mcl-1 resulted in increased myocyte death. As baicalein and SB21 were both cardioprotective, inhibition of the activated GSK-3β–Noxa–Mcl-1 signaling might be involved in the cardioprotection (Figure 8e). The molecular mechanism is unclear, and possible interactions between GSK-3β, Noxa, and Mcl-1 contribute to the myocyte death need further investigation. However, other possibilities cannot be ruled out at present. For example, the larger Zn_i^{2+} release, induced by H_2O_2 or $ONOO^-$ exposure, activated ERK–p53–Noxa-dependent, but GSK-3β-independent, signaling (Figures 7e, 8d and e).

In summary, this study shows that I/R or oxidative and nitrosative stress all induce marked Zn_i^{2+} release, resulting in ERK1/2-activated GSK-3β–p53 and Noxa–Mcl-1 signaling and myocyte death. Inhibition of the reperfusion-induced upstream Zn_i^{2+} release or the use of natural products, flavonoids, are potentially promising strategies for the treatment of cardiac I/R injury.

Materials and Methods

Solutions and chemicals. The Zn_o^{2+}-free normal Tyrode solution used was (in mM): NaCl 118, KCl 4. 5, $MgCl_2$ 1.0, $CaCl_2$ 1.8, glucose 10, and HEPES 10, pH 7.4 at 37 °C. See the Supplemental Materials for the concentration of the reagents used in this study.

Protocols for simulating I/R in cardiomyocytes or I/R in adult-rat hearts

Cultured neonatal ventricular myocytes. All procedures were performed in accordance with the Animal Care Guidelines of the National Taiwan University. The protocol for simulated I/R was modified from that described previously.[4] In brief, myocytes were stabilized in O_2 (21%)-Tyrode solution for 10 min, then were switched to 100% N_2-saturated Tyrode solution for 30 min, followed by reperfusion for 4 h with O_2-Tyrode solution.

Isolated adult-rat hearts. Adult rats were anesthetized and the isolated hearts retrogradely perfused in Langendorff mode. Adult-rat hearts were then subjected to 30 min of global ischemia by halting perfusion, followed by 2 h of reperfusion with Krebs–Henseleit bicarbonate buffer gassed with 95% O_2/5% CO_2 at 37 °C (pH 7.4).

Simultaneous measurement of changes in the $[O_2^{-\bullet}]_i$ and $[Zn^{2+}]_i$ using time-lapse confocal microscopy. A Leica SP confocal laser scanning imaging system (Leica Microsystems, Wetzlar, Germany) equipped with a 63 × oil-immersion objective was used. FluoZin-3 AM (green) and MitoSox Red (red) were co-loaded with MTG into cardiomyocytes to simultaneously detect dynamic changes in the $[O_2^{-\bullet}]_i$ and $[Zn^{2+}]_i$. MitoSox Red is a high affinity and selective fluorescent probe for the $[O_2^{-\bullet}]_i$. TSQ is a non-acetoxymethyl ester Zn^{2+} indicator. Although it is a very sensitive Zn^{2+} probe ($Kd = 10$ nM),[10] it does not depend on cleavage of an acetoxymethyl ester group for uptake and fluorescence, so intracellular TSQ leaks out within a few minutes and it is not possible to measure sequential fluorescent changes.[30] The rest of recording detail, please see Supplemental Methods.

For western blot analysis, siRNA transfection, qPCR measurement, and detection of apoptosis, see the Supplemental Materials.

Statistics. All values are presented as the mean ± SEM of N independent experiments. All data were subjected to one-way ANOVA followed by a *post hoc* test with the Bonferroni's correction. $P < 0.05$ was considered to be statistically significant.

Conflict of Interest

The authors declare no conflict of interest.

Acknowledgements. We gratefully thank the National Science Council of Taiwan for financial support (grants: NSC-98-2320-B-002-042-MY3 and NSC 99-2314-B-166-001-MY3). We also gratefully acknowledge the Second Core Laboratory of Department of Medical Research, National Taiwan University Hospital for expert technical assistance.

1. Maret W, Vallee BL. Thiolate ligands in metallothionein confor redox activity on Zn^{2+} chelators. *Proc Natl Acad Sci* 1998; **95**: 3478–3482.

2. Bozym RA, Thompson RB, Stoddard AK, Fierke CA. Measuring picomolar intracellular exchangeable zinc in PC-12 cells using a ratiometric fluorescence biosensor. *ACS Chem Biol* 2006; **1**: 103–111.
3. Cheung P-Y, Wang W, Schulz R. Glutathione protects against myocardial ischemia-reperfusion injury by detoxifying peroxynitrite. *J Mol Cell Cardiol* 2000; **32**: 1669–1678.
4. Juhaszova M, Zorov DB, Kim S-H, Pepe S, Fu Q, Fishbein KW *et al.* Glycogen synthase kinase-3β mediates convergence of protection signaling to inhibit the mitochondrial permeability transition pore. *J Clin Invest* 2004; **113**: 1535–1549.
5. Yellon DM, Hausenloy DJ. Myocardial Reperfusion Injury. *N Engl J Med* 2007; **357**: 1121–1135.
6. Kang YJ, Li G, Saari JT. Metallothionein inhibits ischemia-reperfusion injury in mouse heart. *Am J Physiol* 1999; **26**: H993–H997.
7. Bossy-Wetzel E, Talantova MV, Lee WD, Schölzke MN, Harrop A, Mathews E *et al.* Crosstalk between nitric oxide and zinc pathways to neuronal cell death involving mitochondrial dysfunction and p38-activated K^+ channels. *Neuron* 2004; **41**: 351–365.
8. Zhang Y, Wang H, Li J, Dong L, Xu P, Chen W *et al.* Intracellular zinc release and ERK phosphorylation are required upstream of 12-lipoxygenease activation in peroxynitrite toxicity to mature rat oligodendrocytes. *J Biol Chem* 2006; **281**: 9460–9470.
9. McIntosh R, Lee SY, Ghio AJ, Xi J, Zhu M, Shen X *et al.* The critical role of intracellular zinc in adenosine A_2 receptor activation induced cardioprotection against reperfusion injury. *J Mol Cell Cardiol* 2010; **49**: 41–47.
10. Karagulova G, Yue Y, Moreyra A, Boutjdir M, Korichneva I. Protective role of intracellular zinc in myocardial ischemia/reperfusion is associated with preservation of protein kinase C isoforms. *JPET* 2007; **321**: 517–525.
11. Sensi SL, Ton-That D, Sullivan PG, Jonas EA, Gee KR, Kaczmarek LK *et al.* Modulation of mitochondrial function by endogenous Zn^{2+} pools. *Proc Natl Acad Sci* 2003; **100**: 6157–6162.
12. Cornell NW, Crivaro KE. Stability constant for the zinc-dithiothreitol complex. *Analy Biochem* 1972; **47**: 203–208.
13. Das S, Wong R, Rajapakse N, Murphy E, Steenbergen C. Glycogen synthase kinase 3 inhibition slows mitochondrial adenine nucleotide transport and regulates voltage-dependent anion channel phosphorylation. *Circ Res* 2008; **103**: 983–991.
14. Gross ER, Hsu AK, Gross GJ. Opioid-Induced cardioprotection occurs via glycogen synthase Kinase β inhibition during reperfusion in intact rat hearts. *Circ Res* 2004; **94**: 960–966.
15. Gomez L, Paillard M, Thibault H, Derumeaux G, Ovize M. Inhibition of GSK-3β by postconditioning is required to prevent opening of the mitochondrial permeability transition pore during reperfusion. *Circulation* 2008; **117**: 2761–2768.
16. Miura T, Miki T. GSK-3β, a therapeutic target for cardiomyocyte protection. *Circ J* 2009; **73**: 1184–1192.
17. Yook JI, Li X-Y, Ota I, Hu C, Kim HS, Kim NH *et al.* A Wnt–Axin2–GSK3β cascade regulates Snail1 activity in breast cancer cells. *Nat Cell Biol* 2006; **8**: 1398–1406.
18. Beurel E, Jope BS. The paradoxical pro-and anti-apoptotic actions of GSK3 in the intrinsic and extrinsic apoptosis signaling pathways. *Prog in Neurobiol* 2006; **79**: 173–189.
19. Lin T, Mak NK, Yang MS. MAPK regulate p53-dependent cell death induced by benzo[a]pyrene: involvement of p53 phosphorylation and acetylation. *Toxicology* 2008; **247**: 145–153.
20. Taylor RC, Cullen SP, Martin SJ. Apoptosis: controlled demolition at the cellular level. *Nat Rev Mol Cell Biol* 2008; **9**: 231–241.
21. Sheridan C, Brumatti G, Elgendy M, Brunet M, Martin SJ. An ERK-dependent pathway to Noxa expression regulates apoptosis by platinum-based chemotherapeutic drugs. *Oncogene* 2010; **29**: 6428–6441.
22. Aikawa T, Shinzawa K, Tanaka N, Tsujimoto Y. Noxa is necessary for hydrogen peroxide-induced caspase-dependent cell death. *FEBS Letters* 2010; **584**: 681–688.
23. Chanoit G, Lee SR, Xi J, Zhu M, McIntosh RA, Mueller RA *et al.* Exogenous zinc protects cardiac cells from reperfusion injury by targeting mitochondrial permeability transition pore through inactivation of glycogen synthase kinase-3β. *Am J Physiol* 2008; **295**: H1227–H1233.
24. Lee SY, Chanoit G, McIntosh R, Zvara DA, Xu Z. Molecular mechanism underlying Akt activation in zinc-induced cardioprotection. *Am J Physiol* 2009; **297**: H569–H575.
25. Eom TY, Roth KA, Jope RS. Neural precursor cells are protected from apoptosis induced by trophic factor withdrawal or genotoxic stress by inhibitors of glycogen synthase kinase 3. *J Biol Chem* 2007; **282**: 22856–22864.
26. Cagnol S, Chambard J-C. ERK and cell death: mechanisms of ERK-induced cell death–apoptosis, autophagy and senescence. *FEBS J* 2010; **277**: 2–21.
27. Kohda Y, Matsunaga Y, Shiota R, Satoh T, Kishi Y, Kawai Y *et al.* Raf-1/Mek/ERK1/2 signaling pathway in zinc-induced injury in rat renal cortical slices. *J Toxicol Sci* 2006; **31**: 207–217.
28. Maurer U, Charvet C, Wagman AS, Dejardin E, Green DR. Glycogen synthase kinase-3 regulates mitochondrial outer membrane permeabilization and apoptosis by destabilization of Mcl-1. *Mol Cell* 2006; **21**: 749–760.
29. Ding Q, He X, Hsu J-M, Xia W, Chen C-T, Li L-Y *et al.* Degradation of Mcl-1 by β-TrCP mediates glycogen synthase kinase 3-induced tumor suppression and chemosensitization. *Mol Cell Biol* 2007; **27**: 4006–4017.
30. Frederickson CJ, Burdette SC, Frederickson CJ, Sensi SL, Weiss JH, Yin HZ *et al.* Method for identifying neuronal cells suffering zinc toxicity by use of a novel fluorescent sensor. *J Neurosci Methods* 2004; **139**: 79–89.

Supplementary Information accompanies the paper on Cell Death and Differentiation website (http://www.nature.com/cdd)